# Bite force estimates in juvenile *Tyrannosaurus rex* based on simulated puncture marks (#58983)



First submission

## Guidance from your Editor

Please submit by **31 Mar 2021** for the benefit of the authors (and your $200 publishing discount) .

**Structure and Criteria**
Please read the 'Structure and Criteria' page for general guidance.

**Raw data check**
Review the raw data.

**Image check**
Check that figures and images have not been inappropriately manipulated.

Privacy reminder: If uploading an annotated PDF, remove identifiable information to remain anonymous.

**Files**
Download and review all files from the materials page.

6 Figure file(s)
1 Table file(s)
1 Raw data file(s)

# Structure and Criteria



## Structure your review

The review form is divided into 5 sections. Please consider these when composing your review:

1. **BASIC REPORTING**
2. **EXPERIMENTAL DESIGN**
3. **VALIDITY OF THE FINDINGS**
4. General comments
5. Confidential notes to the editor

You can also annotate this PDF and upload it as part of your review

When ready submit online.

## Editorial Criteria

Use these criteria points to structure your review. The full detailed editorial criteria is on your guidance page.

### BASIC REPORTING

- Clear, unambiguous, professional English language used throughout.
- Intro & background to show context. Literature well referenced & relevant.
- Structure conforms to PeerJ standards, discipline norm, or improved for clarity.
- Figures are relevant, high quality, well labelled & described.
- Raw data supplied (see PeerJ policy).

### EXPERIMENTAL DESIGN

- Original primary research within Scope of the journal.
- Research question well defined, relevant & meaningful. It is stated how the research fills an identified knowledge gap.
- Rigorous investigation performed to a high technical & ethical standard.
- Methods described with sufficient detail & information to replicate.

### VALIDITY OF THE FINDINGS

- Impact and novelty not assessed. Negative/inconclusive results accepted. *Meaningful* replication encouraged where rationale & benefit to literature is clearly stated.
- All underlying data have been provided; they are robust, statistically sound, & controlled.
- Speculation is welcome, but should be identified as such.
- Conclusions are well stated, linked to original research question & limited to supporting results.

# Standout reviewing tips



The best reviewers use these techniques

| Tip | *Example* |
| --- | --- |
| **Support criticisms with evidence from the text or from other sources** | *Smith et al (J of Methodology, 2005, V3, pp 123) have shown that the analysis you use in Lines 241-250 is not the most appropriate for this situation. Please explain why you used this method.* |
| **Give specific suggestions on how to improve the manuscript** | *Your introduction needs more detail. I suggest that you improve the description at lines 57- 86 to provide more justification for your study (specifically, you should expand upon the knowledge gap being filled).* |
| **Comment on language and grammar issues** | *The English language should be improved to ensure that an international audience can clearly understand your text. Some examples where the language could be improved include lines 23, 77, 121, 128 – the current phrasing makes comprehension difficult. I suggest you have a colleague who is proficient in English and familiar with the subject matter review your manuscript, or contact a professional editing service.* |
| **Organize by importance of the issues, and number your points** | *1. Your most important issue*<br>*2. The next most important item*<br>*3. …*<br>*4. The least important points* |
| **Please provide constructive criticism, and avoid personal opinions** | *I thank you for providing the raw data, however your supplemental files need more descriptive metadata identifiers to be useful to future readers. Although your results are compelling, the data analysis should be improved in the following ways: AA, BB, CC* |
| **Comment on strengths (as well as weaknesses) of the manuscript** | *I commend the authors for their extensive data set, compiled over many years of detailed fieldwork. In addition, the manuscript is clearly written in professional, unambiguous language. If there is a weakness, it is in the statistical analysis (as I have noted above) which should be improved upon before Acceptance.* |

# Bite force estimates in juvenile *Tyrannosaurus rex* based on simulated puncture marks

**Joseph E Peterson** [Corresp., 1], **Z. Jack Tseng** [2], **Shannon Brink** [3]

[1] Department of Geology, University of Wisconsin Oshkosh, Oshkosh, Wisconsin, United States of America

[2] Department of Integrative Biology and Museum of Paleontology, University of California Berkeley, Berkeley, California, United States of America

[3] Department of Geological Sciences, East Carolina University, Greenville, North Carolina, United States of America

Corresponding Author: Joseph E Peterson
Email address: petersoj@uwosh.edu

**Background.** Bite marks attributed to adult *Tyrannosaurus rex* have been subject to numerous studies. However, few bite marks attributed to *T. rex* have been traced to juveniles, leaving considerable gaps in understanding ontogenetic changes in bite mechanics and force, and the paleoecological role of juvenile tyrannosaurs in the late Cretaceous.

**Methods.** Here we present bite force estimates for a juvenile *Tyrannosaurus rex* based on mechanical tests designed to replicate bite marks previously attributed to a *T. rex* of approximately 13 years old. A maxillary tooth of the juvenile *Tyrannosaurus* specimen BMR P2002.4.1 was digitized, replicated in cobalt, and mounted to an electromechanical testing system. The tooth was then pressed into bovine long bones in various locations with differing cortical bone thicknesses at varying speeds for a total of 17 trials. Forces required to replicate punctures were recorded and puncture dimensions were measured.

**Results.** Our experimentally derived linear models suggest bite forces of 4,921.08-6,105.68 N from cortical bone thickness estimated from puncture marks on an *Edmontosaurus* and a juvenile *Tyrannosaurus*. These findings are slightly higher than previously estimated bite forces for a juvenile *Tyrannosaurus rex* of approximately the same size as BMR P2002.4.1 but fall within the expected range when compared to estimates of adult *T. rex*.

# Bite force estimates in juvenile Tyrannosaurus rex based on simulated puncture marks

Joseph E. Peterson1, Z. Jack Tseng2, Shannon Brink3

1 Department of Geology, University of Wisconsin Oshkosh, Oshkosh, WI, USA
2 Department of Integrative Biology and Museum of Paleontology, University of California Berkely, Berkely, CA, USA
3 Department of Geological Sciences, East Carolina University, Greenville, NC, USA

Corresponding Author:
Joseph Peterson1
800 Algoma Blvd, Oshkosh, WI, 54901, USA
Email address: petersoj@uwosh.edu

## Abstract

**Background.** Bite marks attributed to adult *Tyrannosaurus rex* have been subject to numerous studies. However, few bite marks attributed to *T. rex* have been traced to juveniles, leaving considerable gaps in understanding ontogenetic changes in bite mechanics and force, and the paleoecological role of juvenile tyrannosaurs in the late Cretaceous.

**Methods.** Here we present bite force estimates for a juvenile *Tyrannosaurus rex* based on mechanical tests designed to replicate bite marks previously attributed to a *T. rex* of approximately 13 years old. A maxillary tooth of the juvenile *Tyrannosaurus* specimen BMR P2002.4.1 was digitized, replicated in cobalt, and mounted to an electromechanical testing system. The tooth was then pressed into bovine long bones in various locations with differing cortical bone thicknesses at varying speeds for a total of 17 trials. Forces required to replicate punctures were recorded and puncture dimensions were measured.

**Results.** Our experimentally derived linear models suggest bite forces of 4,921.08-6,105.68 N from cortical bone thickness estimated from puncture marks on an *Edmontosaurus* and a juvenile *Tyrannosaurus*. These findings are slightly higher than previously estimated bite forces for a juvenile *Tyrannosaurus rex* of approximately the same size as BMR P2002.4.1 but fall within the expected range when compared to estimates of adult *T. rex*.

## Introduction

Bite mechanics and feeding habits of dinosaurs have long been debated. A variety of methods have been proposed to determine the bite mechanics and forces of members of

Dinosauria, including stegosaurs, ceratopsians and hadrosaurids (Weishampel, 1984; Bell et al., 2009; Reichel, 2010; Erickson et al., 2015), and more commonly, theropods (Rayfield et al., 2001; Rayfield et al., 2005; Rayfield et al., 2007; Gignac et al., 2010; Lautenschlager et al., 2013). The genus *Tyrannosaurus rex* and other tyrannosaurids have famously been the focus of many studies on dinosaur bite force and bite mechanics (Erickson et al., 1996; Meers, 2002; Barret and Rayfield, 2006; Bates and Falkingham, 2012; Gignac and Erickson, 2017; Rowe and Snively, 2021; Therrien et al., 2021). These studies have relied on several methods for estimating bite forces, including multi-body dynamic analysis (MDA) (Bates and Falkinham, 2012), finite element analysis (Rayfield et al., 2005; Rayfield et al., 2007; Maiorino et al., 2015), and actualistic studies.

However, bite force estimates have largely focused on adult specimens with few studies providing estimates for juveniles or subadult *Tyrannosaurus rex*, leaving a considerable gap in the understanding of tyrannosaur ontogenetic dietary partitioning and paleoecology. Bates and Falkingham (2012) based their bite force estimate of a late-stage juvenile *T. rex* on multi-body dynamic analysis (MDA), suggesting allometric growth in bite force from juvenile to adult. The juvenile specimen used in that study (BMRP2002.4.1) was also found to possess conspecific bite marks through the left maxilla and nasal (Peterson et al., 2009) (Figure 1A-E). Similarly, Peterson and Daus (2019) identified feeding traces on a proximal caudal vertebra from an *Edmontosaurus* likely produced by a *T. rex* of a similar ontogenetic stage (Figure 2A-E). The trace on BMR P2002.4.1 penetrates through 7.5 mm of cortical bone, while the traces on BMR P2007.4.1 penetrates through 0.4 mm of cortical bone. Both sets of puncture marks are approximately 10-19 mm in length, and 4-9 mm in width (Peterson et al, 2009; Peterson and Daus, 2019).

The presence of two sets of puncture marks attributable to a late-stage juvenile *Tyrannosaurus rex* provides the opportunity to test previously derived juvenile *T. rex* bite force estimates from multi-body dynamic analyses with actualistic methods (Gignac et al., 2010). Comparisons between the bite forces of adult and juvenile *Tyrannosaurus rex* ~~has~~ the potential to reveal ontogenetic niche partitioning (Woodward et al., 2020) and illuminate the impact of *Tyrannosaurus rex* ontogeny in terrestrial Cretaceous ecosystems.

## Materials & Methods

Gignac et al. (2010) reported on bite marks in a specimen of *Tenontosaurus tilletti* that were attributed to *Deinonychus antirrhopus,* and designed indentation experiments to determine bite force estimates for *D. antirrhopus*. ~~T~~o estimate the bite force for a juvenile *Tyrannosaurus*, ~~we used similar methods.~~ Previous studies of BMR P2002.4.1 and BMR P2007.4.1 suggest that their respective bite marks were produced by a lateral maxillary tooth of a juvenile to sub-adult tyrannosaur (Peterson et al., 2009; Peterson and Daus, 2019). To replicate these indentations, a lateral maxillary tooth of the juvenile *Tyrannosaurus* specimen BMR P2002.4.1 was digitized and 3D printed. Triangulated laser texture scans were conducted at the Department of Geology at the University of Wisconsin-Oshkosh in Oshkosh, WI. Scans were made with a NextEngine 3D Laser Scanner, capturing data at seven scanning divisions in high definition (2.0k points/in2). Models were built with the NextEngine ScanStudio HD Pro version 2.02 and finalized as STL models (Figure 3A). The STL files were then imported into Meshmixer (Autodesk, version 10.0.297), in which the 'Make Solid' algorithm was utilized to prepare the model for printing by filling 'gaps' in the model mesh as well as the removal of artifacts from the scanning process (Peterson and Krippner, 2019). The digital model of the tooth was then fused to a model of an adapter that allowed the 3D printed model to be mounted onto the test frame (see below) using

Geomagic Wrap (3D Systems, Cary, NC). The STL file was 3D printed in a dental grade cobalt chromium alloy [Co(61.0),Cr(25.0),Mo(6.0),W(5.0),Mn(<1.0),Si(<1.0), Fe(<1.0)] with a yield strength of 47,436 N/cm$^2$ (Figure 3B) by the Argen corporation (San Diego, CA).

The cobalt chromium alloy tooth model was mounted to a Shimadzu AGS-X Universal Electromechanical Test Frame (ETF) equipped with a 10kN load cell, interfaced with the Shimadzu TrapeziumX software for data collection. Prior experiments on bite force determination have utilized bovine limb bones for their varying cortical thicknesses and similarity in microstructure to dinosaurian elements (Erickson et al, 2002; Locke, 2004; Gignac et al., 2010). While the elements under study include cranial and vertebral elements that may differ in microstructure than limb elements, the comparable variance in cortical thickness makes bovid limb elements suitable models for these experiments.

A right bovine humerus and an in-tact left radius/ulna pair, sourced from Moriarty Meats located at 1650 Elmwood Ave, Buffalo, NY 14207 were used for indent simulations. The bones were kept frozen upon purchase and thawed overnight at room temperature before testing proceeded. Epiphyses were left in-tact to reduce the possibility of creating microfractures and compromising structural integrity during removal. Bones were covered with paper towels soaked in Hank's Balanced Salt Solution (HBSS) between tests to maintain moisture. The bones were secured to the lower stage of the ETF using a series of 1-inch width nylon straps. Testing parameters including maximum allowed force (10kN), maximum displacement (ranging from 5-45mm depending on depth of the test location on specimen), and speed (1 mm/s) were set. The tooth model was then pressed into the bones in various locations with differing cortical bone thicknesses to produce a total of 17 indents (Figure 4A, B). After each individual test, the resulting indent was measured using Mitutoyo vernier calipers for depth, width, and length to the

nearest 0.02 mm before proceeding. We plotted load-displacement relationships of all trials runs and kept only trials with smooth curves as in Gignac et al. (2010); curves that exhibited sudden drops in measured load indicate presence of fractures at and around the indentation site, and those curves were excluded from subsequent analyses. Post-indent testing, all specimens were scanned at 0.6 mm slice thickness using a GE Discovery 690 PET-CT scanner in the University at Buffalo Clinical and Translational Science Institute Image Center (Figure 5).

To estimate the indentation forces required to make the specific puncture marks observed on BMR P2007.4.1 and BMR P2002.4.1, we used linear regression to model the relationship between per trial maximum recorded indentation force and puncture site cortical bone thickness, as in Gignac et al. (2010). We then used the linear regression model to calculate the indentation forces required to make puncture marks with the measured cortical thickness values from BMR P2007.4.1 (0.4 mm) and BMR P2002.4.1 (7.5 mm). Additionally, we estimated the uncertainty around the calculated indentation forces using 95% confidence intervals around the linear regression model equation. These calculations were conducted in the R programming environment using the core functions *lm* and *predict*.

## Results

The trial data were analyzed using linear modeling of bovine specimen cortical thickness and indentation force values and derived predictive formulae (1) with the full data set and (2) with fractured trial values excluded (Fig. 6A-B). The results indicate a mean force of 1,412.79-2,292.46N for the indentation on BMR P2007.4.1 (“Constantine”) and 4,921.08-6,105.68N for the indentations on BMR P2002.4.1 (“Jane”) (Table 1).

The maximum force recorded by the 10kN load cell was 10,448.60 N, and minimum 782.93 N (mean force: 4,430.63 N). Summary of each trial and raw force-displacement time

series data are available as supplemental data (S1-S2). A video of one of the experimental trials and CT images of the experimentally punctured cow elements are available on MorphoSource (S3-S4) (https://www.morphosource.org/Detail/ProjectDetail/Show/project_id/1117).

## Discussion

Estimated bite forces of adult *Tyrannosaurus rex* have yielded a wide range of results, and our study provides the first experimentally derived juvenile bite force estimates to contextualize the assessment of adult bite force estimates. Modelled muscle volume estimates for adult *T. rex* bite correspond to forces between 8,526 and 34,522 N (Barrett and Rayfield, 2006; Bates and Falkingham, 2012). However, estimates incorporating likely muscle fiber length produced results over 64,000 N for adult *T. rex* (Bates and Falkingham, 2018). Furthermore, the unique tooth morphology and arrangement in adult *T. rex* promote fine fragmentation of bone during osteophagy (Gignac and Erickson, 2017). Juvenile *T. rex* such as BMR P2002.4.1 have much narrower and blade-like tooth morphologies (Carr, 2020) and were unlikely to have been able to withstand similar bite forces at this ontogenetic stage. Bates & Falkingham (2012) estimated a maximum bite force for BMR P2002.4.1 at 2,400-3,850 N and hypothesized that ontogenetic increases in bite force could indicate a change in dietary partitioning and feeding behavior while approaching adulthood. Our experimentally derived linear models suggest bite forces of 4,921.08-6,105.68 N from cortical bone thickness estimated from puncture marks on *Edmontosaurus* (BMR P2007.4.1) and a juvenile *Tyrannosaurus* (BMR P2002.4.1). These results suggest indentation forces substantially greater than previous estimates for juveniles.

The testing equipment used in this study has a limit of 10,000 N. However, most of the results were well below this limit, suggesting that mechanical limits of the equipment were not a factor in the results. Furthermore, the load cell on the test frame is rated for 10,000 N, with a

built-in safety factor of ~5% over the listed limit. Therefore, it is possible that the values at and over 10,000 N may be truncated. To assess the effect of potential truncation bias on our linear model estimates of indentation force, we repeated the analysis by excluding force values at and over 10,000 N; the resulting indentation force estimates for the fossilized bite marks vary by 16-17% (higher in the "Constantine" specimen with trimmed data, lower in the "Jane" specimen with trimmed data). Conservative adjustment of all model-predicted indentation forces by a factor of 17% on both ends still returns values higher than previous estimates (4084.50-5067.71 N with 17% adjustment vs. 2,400-3,850 N reported by Bates & Falkingham).

Bone mechanical behavior is loading rate-dependent, with increasing strength at higher loading rates (McElhaney 1966). To gain a broader context for the standardized loading rate used in our experiments (1 mm/s), we conducted a limited number of bone puncture trials at 10 mm/s (n = 3 trials) and 16 mm/s (n = 2 trials, presenting the maximum speed permitted on the equipment used). The resulting relationships between puncture force and cortical thickness at puncture site in this small sample of additional trials are consistent with those obtained from the 1 mm/s trials. At 10 mm/s, cortical thicknesses ranging from 3.7 to 5.3 mm required forces of 2930.4 to 10,448.6 N. At 16 mm/s, a cortical thickness of 4.5 mm correlated with a puncture force of 3248.8 N, and a thickness of 9 mm correlated with 9024.41 N. The range of material properties present (not quantified) throughout the test samples may be partially responsible for the variability in puncture forces measured at a given cortical thickness, and explain the similar results obtained in this study using different puncture rates (i.e., higher loading rates at less stiff locations may result in similar required puncture forces as low loading rates at stiffer locations on the bone sample).

Most of the force-displacement curves from experimental trials exhibit a stereotypical linear or near-linear initial portion, consistent with expectations from first principles of bone mechanics within the elastic region of a material force-displacement or stress-strain curve. In contrast, all but three of the force-displacement curves exhibited no clear peak force/stress; instead, the bone puncture continued to enlarge with additional penetration depth, with oscillating force magnitudes (data not shown) (Erickson et al., 2004; Gignac et al.,2010). While these results do not permit absolute determination of whether the bites studied were made with the animals' highest possible bite force, they do offer insight into the minimum boundary for the bite force capabilities of a late-stage juvenile *Tyrannosaurus rex*.

We observed that the irregularly shaped epiphyses of the bovine bone specimens sometimes generated minor to substantial movements of the test specimen relative to the testing frame during bite trials, despite the use of nylon straps to secure the specimens. Test trials that exhibited visible movements of the bone were removed from data analysis, but it is likely that minute movements took place during some of the bite force experiments. Consequently, we did not discuss the bite force trials individually, and we instead relied on mean and range values as more robust estimates of the bite force values used in our linear model-based estimates of bite force, which were in turn based on cortical bone thickness at puncture mark sites of fossil specimens. The possible movement of bone specimens during a given bite experiment is not an unrealistic factor in the actual feeding and predatory behavior being studied, as movements of multiple bodies are involved in generating puncture marks from agonistic or hunting behavior in predators. Future studies that include a more formalized consideration of potential multibody dynamics of a particular bite would provide further refinement on such bite force estimates. We opted to maintain the unmodified state of bone specimens in our trials, rather than processing

those samples into standardized shapes (e.g., cubes, cylinders), in order to minimize inadvertent damage to samples from cutting and to maximize the number of testing locations on each specimen. As such, the flexure of specimens is considered alongside flexures of the components of the testing frame itself as systematic errors in the study design that added variability to our measured values. Accordingly, the reported findings should be considered in this context.

The tooth marks observed on BMR P2002.4.1 and BMR P2007.4.1 are Type 1 punctures (Jacobsen, 1998; Tanke and Currie, 1998), described as "*punctures (partial and full penetration) are circular to oval in outline. In unhealed examples, plates of bone are folded down and inwards into the puncture hole. The tooth/teeth are pushed into the bone and extracted with no additional damage*" (Jacobsen, 1998). Erickson and Olson (1996) note that the tooth marks most attributed to *T. rex* are classified as Type 1 and Type 2 ("*Transverse gouges, scores or tooth drag imprints are elongate, gently curving lesions with ragged (or healing) margins*" which are also known as "pull and puncture") (Erickson et al., 2004; Carr, 2020).

Similar Type 1 punctures have been observed on the skulls of fossil and extant crocodiles (Buffetaut, 1983; Katsura, 2004; Peterson et al., 2009) and attributed to intraspecific fighting. Intraspecific facial biting in crocodylians involves rapid single bites to the face with quick inertial movements (Kalin, 1939; Webb and Messel, 1977; Webb et al., 1983; Bramble and Wake, 1985; Lang, 1987; Cleuren and De Vree, 2000; Schwenk, 2000; Njau and Blumenschine, 2006; Hiiemae and Crompton, 2013). Injuries from intraspecific aggression have also been observed in juvenile Cinereous Vultures (*Aegypius monachus*) and Griffon Vultures (*Gyps fluvus*) (Blanco et al., 1997).

Feeding behaviors in crocodylians involve similar sequences of biting and quick inertial movements (Cleuren and De Vree, 2000; Njau and Blumenschine, 2006; Noto et al., 2012).

However, during feeding carcasses are commonly dismembered through more vigorous inertial movements such as “death-rolling” where the predator will spin its body along the longitudinal axis while gripping the carcass in its jaws (Schmidt, 1944; Attwell, 1959; Green, 1988; Njau and Blumenschine, 2006). This method of carcass reduction permits inertial feeding and often produces abundant and deep-penetrating tooth marks that are morphologically similar to Type 1 and Type 2 tooth marks observed in theropod dinosaurs (Njau and Blumenschine, 2006).

Bite marks and feeding traces attributed to theropod dinosaurs have been extensively studied (Fiorillo, 1991; Carpenter, 1998; Chure et al., 1998; Jacobsen, 1998; Tanke and Currie; 1998; Farlow and Holtz, 2002; Fowler and Sullivan, 2006; Happ, 2008; Bell and Currie; 2009; Peterson et al., 2009;Gignac et al., 2010; Peterson and Daus, 2019; Eberth and Currie, 2010; Hone and Rauhut; 2010; Hone and Watabe, 2010; Longrich et al., 2010; DePalma et al., 2013; Hone and Tanke, 2015; McLain, 2018; Drumheller et al., 2020). Whereas most studies discuss tooth marks attributable to adult theropods, the ability to observe multiple bitten specimens from a juvenile offer insight into potential ontogenetic shifts in diet and behavior. Bite marks specifically attributable to intraspecific aggression in theropods include Type 1 and Type 2 tooth marks to the maxilla, nasal, jugal, and dentary (Tanke and Currie, 1998; Bell and Currie, 2009; Peterson et al., 2009). In crocodylians, these injuries are produced during rapid biting motions directed at the face, which is covered in relatively thin integument and tissues, requiring less resistance from muscle prior to striking bone.

Alternatively, traces from feeding can occur in a wide variety of skeletal locations, and the amount of soft tissue present at the time of the bite can have considerable ramifications for the morphology of the bite mark. For example, the bitten caudal vertebra of BMR P2007.4.1 is from the cranial-most part of the tail where substantial muscles such as the M. ilio-ischocaudalis

and M. caudiofemoralis longus would have been present in life (Snively and Russell, 2007; Peterson and Daus, 2019). However, the punctures are present on the ventral surface of the centrum, suggesting that the tyrannosaur was feeding after the haemal complexes and most of the superficial hypaxial muscles and M. caudofemoralis longus had been removed (Peterson and Daus, 2019). Despite the inferred later-stage feeding, the punctures on BMR P2007.4.1 still penetrate approximately 5mm in depth. Similar penetrating marks occur from crocodylians during the disarticulation of a carcass (i.e. "death-rolling"). The modelled craniocervical musculature of adult *Tyrannosaurus rex* (based on analysis of superficial muscular reconstructions of the M. transversospinalis capitis, M. complexus, and M. longissimus capitis superficialis) suggest rapid strikes and inertial feeding similar to what is seen in extant archosaurs (Snively and Russell, 2007). As such, the feeding traces present on BMR P.2007.4.1 may have been the result of dismemberment of the carcass by a juvenile tyrannosaur.

These experimental reconstructions of the punctures present on BMR P2002.4.1 and BMR P2007.4.1 suggest that late-stage juvenile and subadult tyrannosaurs were capable of puncturing bone during feeding and intraspecific aggressive bouts despite the absence of the large, blunt dental crowns of adults (Woodward et al., 2020). The tooth marks present on BMR P2007.4.1 are consistent with feeding traces during dismemberment, possibly while a significant amount of soft tissue was still present (Peterson and Daus, 2019). Alternatively, the facial pathologies on BMR P2002.4.1 involved minimal tissue, thus a quicker, higher-inertia bite is likely, consistent with intraspecific aggression in crocodylians (Njau and Blumenschine, 2006; Peterson et al., 2009). Further identification of tyrannosaur feeding traces from different ontogenetic stages may reveal more insight into the ecological role and potentially dynamic dietary trends and of *Tyrannosaurus rex* throughout ontogeny.

## Acknowledgements

The authors thank thank William W. Brink for laboratory assistance during experimentation trials, Drs. Jonathan P. Warnock, Christopher R. Noto, and Stephanie K. Drumheller-Horton for stimulating discussion in the experimental design. We that Drs. M. Allison Stegner and Jonathan P. Warnock for constructive feedback on an early version of this manuscript. We also thank Paul Cascone and the Argen Corporation for assisting in the production of the cobalt tooth model used in this study. CT scanning was in part supported by the National Center for Advancing Translational Sciences of the National Institutes of Health under award number UL1TR001412 to the University at Buffalo.

## References

Attwell RIG/ 1958. Crocodiles at Carion. Afr. Wildl. 13:13-22.

Barrett P. and Rayfield E. 2006. Ecological and evolutionary implications of dinosaur feeding behaviour. Trends. Ecol. Evol. 21:217–224.

Bates KT and Falkingham PL. 2012. Estimating maximum bite performance in *Tyrannosaurus rex* using multi-body dynamics. Biol. Letters. 8:660–664.

Bates KT and Falkingham PL. 2018. The importance of muscle architecture in biomechanical reconstructions of extinct animals: a case study using *Tyrannosaurus rex*. J. Anat. 233:625–635.

Bell PR and Currie PJ. 2009. A tyrannosaur jaw bitten by a confamilial: scavenging or fatal agonism? Lethaia. 43:278–281.

Bell PR, Snively E, and Shychoski LA. 2009. Comparison of the jaw mechanics in hadrosaurid and ceratopsid dinosaurs using finite element analysis. Anat. Rec. 292:1338–1351.

Blanco G, Traverso JM, Marchamalo J, and Martinez F. 1997. Interspecific and intraspecific aggression among Griffon and Cinereous Vultures at nesting and foraging sites. J. Raptor. Res. 31:77-79.

Bramble DM and Wake D. 1985. Feeding mechanisms of lower tetrapods. In: Hildebrand M, Bramble D, Liem K, and Wake D, eds. *Functional Vertebrate Morphology.* Cambridge: Harvard University Press, 230-261.

Buffetaut E. 1983. Wounds on the jaw of an eocene mesosuchian crocodilian as possible evidence for the antiquity of crocodilian intraspecific fighting behaviour. PalZ. 57:143–145.

Carpenter K. 1998. Evidence of predatory behavior by carnivorous dinosaurs. Gaia. 15:135-144.

Carr TD. 2020. A high-resolution growth series of *Tyrannosaurus rex* obtained from multiple lines of evidence. PeerJ. 8, 9192; 10.7717/peerj.9192.

Chure D.J, Fiorillo AR, and Jacobsen A. 1998. Prey bone utilization by predatory dinosaurs in the Late Jurassic of North America, with comments on prey bone use by dinosaurs throughout the Mesozoic. Gaia. 15:227-232.

Cleuren J and De Vree F. 2000. Feeding in crocodilians. In: Schwenk K, ed. *Feeding: Form, Function, and Evolution in Tetrapod Vertebrates*. San Diego: Academic Press, 337-358.

DePalma RA, Burnham DA, Martin LD, Rothschild BM, and Larson PL. 2013. Physical evidence of predatory behavior in *Tyrannosaurus rex*. P. Natl. Acad. Sci. USA. 110:12560–12564.

Drumheller SK, Mchugh JB, Kane M, Riedel A, and D'Amore DC. 2020. High frequencies of theropod bite marks provide evidence for feeding, scavenging, and possible cannibalism in a stressed Late Jurassic ecosystem. Plos. One. 15, 0233115; 10.1371/journal.pone.0233115.

Eberth DA and Currie PJ. 2010. Stratigraphy, sedimentology, and taphonomy of the *Albertosaurus* bonebed (upper Horseshoe Canyon Formation; Maastrichtian), southern Alberta, Canada. Can. J. Earth. Sci. 47:1119–1143.

Erickson GM and Olson KH. 1996. Bite marks attributable to *Tyrannosaurus rex*: preliminary description and implications. J. Vertebr. Paleontol. 16:175–178.

Erickson GM, Van Kirk SD, Su J, Levenston ME, Caler WE, and Carter DR. 1996. Bite-force estimation for *Tyrannosaurus rex* from tooth-marked bones. Nature. 382:706–708.

Erickson GM, Sidebottom MA, Kay DI, Turner KT, Ip N, Norell MA, Sawyer WG, and Krick BA. 1996. Wear biomechanics in the slicing dentition of the giant horned dinosaur *Triceratops*. Sci. Adv. 1, 1500055; 10.1126/sciadv.1500055.

Erickson GM, Catanese J III, and Keaveny T. 2002. Evolution of the biomechanical material properties of the femur. Anat. Rec. 268:115–124.

Erickson GM, Lappin AK, Parker T, and Vliet KA. 2004. Comparison of bite-force performance between long-term captive and wild American alligators (*Alligator mississippiensis*). J. Zool. 262:21–28.

Farlow JO and Holtz TR. 2002. The fossil record of predation in dinosaurs. The Paleontological Society Papers 8:251–266.

Fiorillo AR. 1991. Prey bone utilization by predatory dinosaurs. Palaeogeogr. Palaeoclimatol. Palaeoecol. 88:157–166.

Fowler DW and Sullivan RWM. 2006. A ceratopsid pelvis with toothmarks from the Upper Cretaceous Kirtland Formation, New Mexico: evidence of late Campanian tyrannosaurid feeding behavior. New Mexico Museum of Natural History and Science Bulletin. 35:127-130.

Gignac PM and Erickson GM. 2017. The biomechanics behind extreme osteophagy in *Tyrannosaurus rex*. Sci. Rep. 7, 2012. doi.org/10.1038/s41598-017-02161-w.

Gignac PM, Makovicky PJ, Erickson GM, and Walsh RP. 2010. A description of D*einonychus antirrhopus* bite marks and estimates of bite force using tooth indentation simulations. J. Vertebr. Paleontol. 30:1169–1177.

Green J. 1988. Crocodile 1: Go ahead make his day. Geo. 9:17-29.

Happ J. 2008. An analysis of predator-prey behavior in a head-to head encounter between *Tyrannosaurus rex* and *Triceratops*. In: Larson P and Carpenter K, eds. *Tyrannosaurus rex the Tyrant King*. Bloomington: Indiana University, 352–370.

Hiiemae KM and Crompton AW. 2013. Mastication, food transport and swallowing. In: Hildebrand M, Bramble D, Liem K, and Wake D, eds. *Functional Vertebrate Morphology*. Cambridge: Harvard University Press, 262-290.

Hone DWE and Tanke DH. 2015. Pre- and postmortem tyrannosaurid bite marks on the remains of *Daspletosaurus* (Tyrannosaurinae: Theropoda) from Dinosaur Provincial Park, Alberta, Canada. PeerJ. 3, 885; 10.7717/peerj.885.

Hone DWE and Watabe M. 2010. New information on the scavenging and selective feeding behavior of tyrannosaurids. Acta. Paleontol. Pol. 55:627-634.

Hone DWE and Rauhut OWM. 2010. Feeding behaviour and bone utilisation by theropod dinosaurs. Lethia. 43:232-244.

Jacobsen AR. 1998. Feeding behaviour of carnivorous dinosaurs as determined by tooth marks on dinosaur bones. Hist. Biol. 13:17–26.

Kalin JA. 1936. Uber Skeletanomalien der Crocodilien: Zeitschrift fur Morphologie und Oekologie de Tiere 32 :327-347.

Katsura Y. 2004. Paleopathology of *Toyotamaphimeia machikanensis* (Diapsida, Crocodylia) from the middle Pleistocene of central Japan. Hist. Biol. 16:93–97.

Lang W. 1987. Crocodilian behavior: implications for management. In: Webb GJW, Manolis SC, and Whitehead PJ, eds. *Wildlife Management: Crocodiles and Alligators*. Syndey: Surrey Beatty, 273-294.

Lautenschlager S, Witmer LM, Altangerel P, and Rayfield EJ. 2013. Edentulism, beaks, and biomechanical innovations in the evolution of theropod dinosaurs. P. Nat. Acad. Sci. 110:20657–20662.

Locke M. 2004. Structure of long bones in mammals. Journal of Morphology. 262:546-565.

Longrich NR, Horner JR, Erickson GM, and Currie PJ. 2010. Cannibalism in *Tyrannosaurus rex*. Plos. One. 5, 0012314; 10.1371/journal.pone.0013419.

Maiorino L, Farke AA, Kotsakis T, Teresi L, and Piras P. 2015. Variation in the shape and mechanical performance of the lower jaws in ceratopsid dinosaurs (Ornithischia, Ceratopsia). J. Anat. 227:631–646.

McElhaney JH. 1966. Dynamic response of bone and muscle tissue. J. Appl. Physiol. 21:1231–1236.

McLain MA, Nelsen D, Snyder K, Griffin CT, Siviero B, Brand LR, and Chadwick AV. 2018. Tyrannosaur cannibalism: a case of a tooth-traced tyrannosaurid bone in the Lance Formation (Maastrichtian), Wyoming. Palaios. 33:164-173.

Meers MB. 2002. Maximum bite force and prey size of *Tyrannosaurus rex* and their relationships to the inference of feeding behavior. Hist. Biol. 16:1–12.

Njau JK and Blumenschine RJ. 2006. A diagnosis of crocodile feeding traces on larger mammal bone, with fossil examples from the Plio-Pleistocene Olduvai Basin, Tanzania. J. Hum. Evol. 50:142–162.

Noto CR, Main DJ, and Drumheller SK. 2012. Feeding traces and paleobiology of a Cretaceous (Cenomanian) crocodyliform: example from the Woodbine Formation of Texas. Palaios. 27:105-115.

Peterson JE and Daus KN. 2019. Feeding traces attributable to juvenile *Tyrannosaurus rex* offer insight into ontogenetic dietary trends. PeerJ. 7,6573; 10.7717/peerj.6573.

Peterson JE and Krippner ML. 2019. Comparisons of fidelity in the digitization and 3D printing of vertebrate fossils. Journal of Paleontological Techniques. 22:1-9.

Peterson JE, Henderson MD, Scherer RP, and Vittore CP. 2009. Face biting on a juvenile tyrannosaurid and behavioral implications. Palaios. 24:780–784.

Rayfield EJ. 2005. Aspects of comparative cranial mechanics in the theropod dinosaurs *Coelophysis*, *Allosaurus* and *Tyrannosaurus*. Zool. J. Linn Society. 144:309–316.

Rayfield EJ, Norman DB, Horner CC, Horner JR, Smith PM, Thomason JJ, and Upchurch P. 2001. Cranial design and function in a large theropod dinosaur. Nature. 409:1033–1037.

Rayfield EJ, Milner AC, Xuan VB, and Young PG. 2007. Functional morphology of spinosaur 'crocodile-mimic' dinosaurs. J. Vertebr. Paleontol. 27:892–901.

Reichel MA. 2010. Model for the bite mechanics in the herbivorous dinosaur *Stegosaurus* (Ornithischia, Stegosauridae). Swiss. J. Geosci. 103:235–240.

Rowe AJ and Snively E. 2021. Biomechanics of juvenile tyrannosaurid mandibles and their implications for bite force. Anatomical Record. doi.10.1002/ar.24602.

Schimdt KP. 1944. Crocodiles. Fauna. 6:67-72.

Schwenk K. 2000. An introduction to tetrapod feeding. In: Schwenk K, ed. *Feeding: Form, Function, and Evolution in Tetrapod Vertebrates*. San Diego: Academic Press, 21-61.

Sharir A, Barak MM, and Shahar R. 2008. Whole bone mechanics and mechanical testing. The Veterinary Journal. 177:8-17.

Snively E and Russell AP. 2007. Functional morphology of neck musculature in the Tyrannosauridae (Dinosauria, Theropoda) as determined via a hierarchical inferential approach. Zool. J. Linn. Soc-London. 151:759–808.

Tanke DH andCurrie PJ. 1998. Head-biting behavior in theropod dinosaurs: paleopathological evidence. Gaia. 15:167-184.

Therrien F, Zelenitsky DK, Voris JT, and Tanaka K. 2021. Mandibular force profiles and tooth morphology in growth series of *Albertosaurus sarcophagus* and *Gorgosaurus libratus* (Tyrannosauridae: Albertosaurinae) provide evidence for an ontogenetic dietary shift in tyrannosaurids. Canadian Journal of Earth Science. doi.org/10.1139/cjes-2020-0177.

Webb G and Messel H. 1977. Abnormalities and injuries in the estuarine crocodile *Crocodylus porosus*. Wildlife. Res. 4:311-391.

Webb G, Manolis S, and Buckworth R. 1983. *Crocodylus johnstoni* in the McKinlay River area N.T, V. Abnormalities and injuries. Wildlife. Res. 10:407-420.

Weishampel DB. 1984. Ornithopod jaw mechanics. In: Weishampel DB, ed. *Evolution of Jaw Mechanisms in Ornithopod Dinosaurs*. Advances in Anatomy Embryology and Cell Biology 87. Berlin: Springer Heidelberg.

Woodward HN, Tremaine K, Williams SA, Zanno LE, Horner JR, and Myhrvold N. 2020. Growing up *Tyrannosaurus rex*: osteohistology refutes the pygmy "*Nanotyrannus*" and supports

489 ontogenetic niche partitioning in juvenile *Tyrannosaurus*. Sci. Adv. 6, 6250;
490 10.1126/sciadv.aax6250.
491

# Figure 1

Lesions present on the face of BMR P2002.4.1.

A) A line drawing of the lesions (1–4). B) Red arrows indicate the locations of the four lesions on the left maxilla and nasal of BMR P2002.4.1. C) A dorsal view of the anterior nasal, red arrow indicating asymmetry resulting from the puncture on the left side. D) The first puncture (arrow 5 lesion 1) located on the articular surface of the anterior nasal and left maxilla. E) The three lesions on the left maxilla of BMR P2002.4.1 with a close-up of lesion 4 (F). Scale bars: A–B 5 10 cm; C–E 5 5 cm. Figure modified from Peterson et al., 2009.

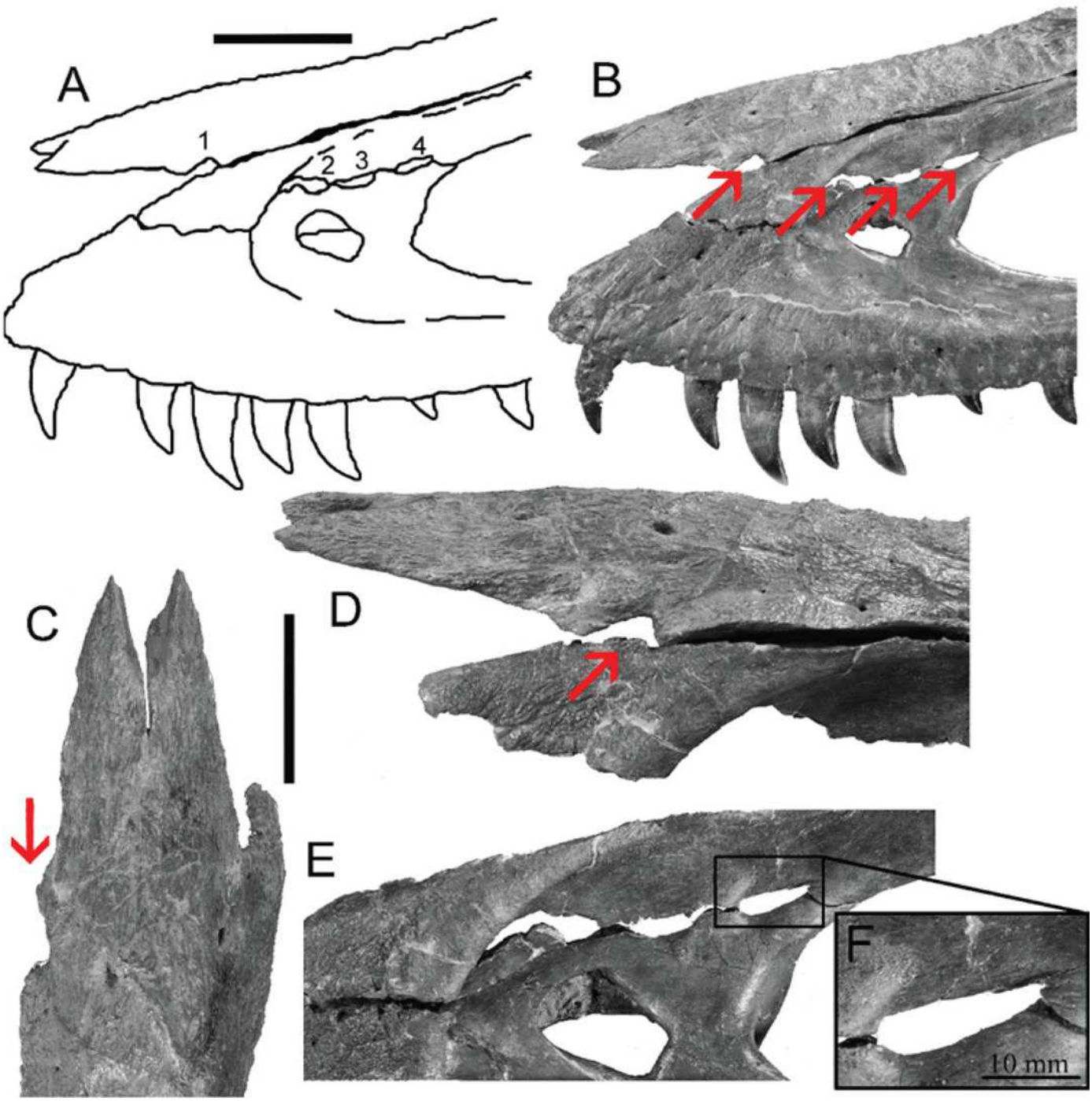
A
1
2
3
4
B
C
D
E
F
10 mm

# Figure 2

Punctured caudal vertebra of BMR P2007.4.1.

Punctured caudal vertebra of BMR P2007.4.1. BMR P2007.4.1 in (A) anterior, (B) posterior, and (C) ventral views, including (D, E) the two elliptical punctures on the ventral surface of the centrum. Modified from Peterson and Daus, 2019.

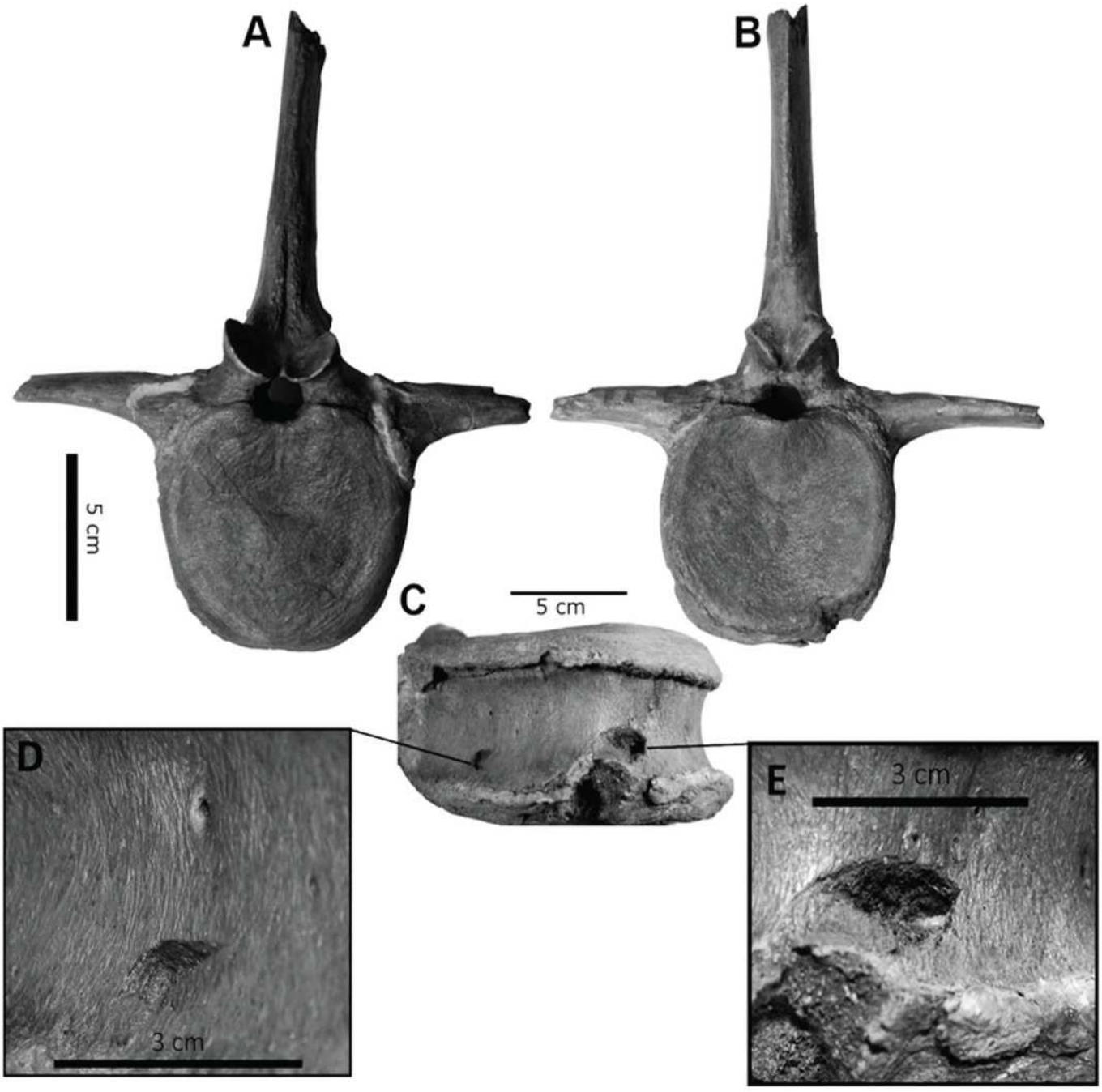
A
B
5 cm
C
5 cm
D
3 cm
E
3 cm

# Figure 3

Maxillary tooth model of BMR P2002.4.1.

A) digital model, and B) 3D print in cobalt used for bite force simulation experiments.

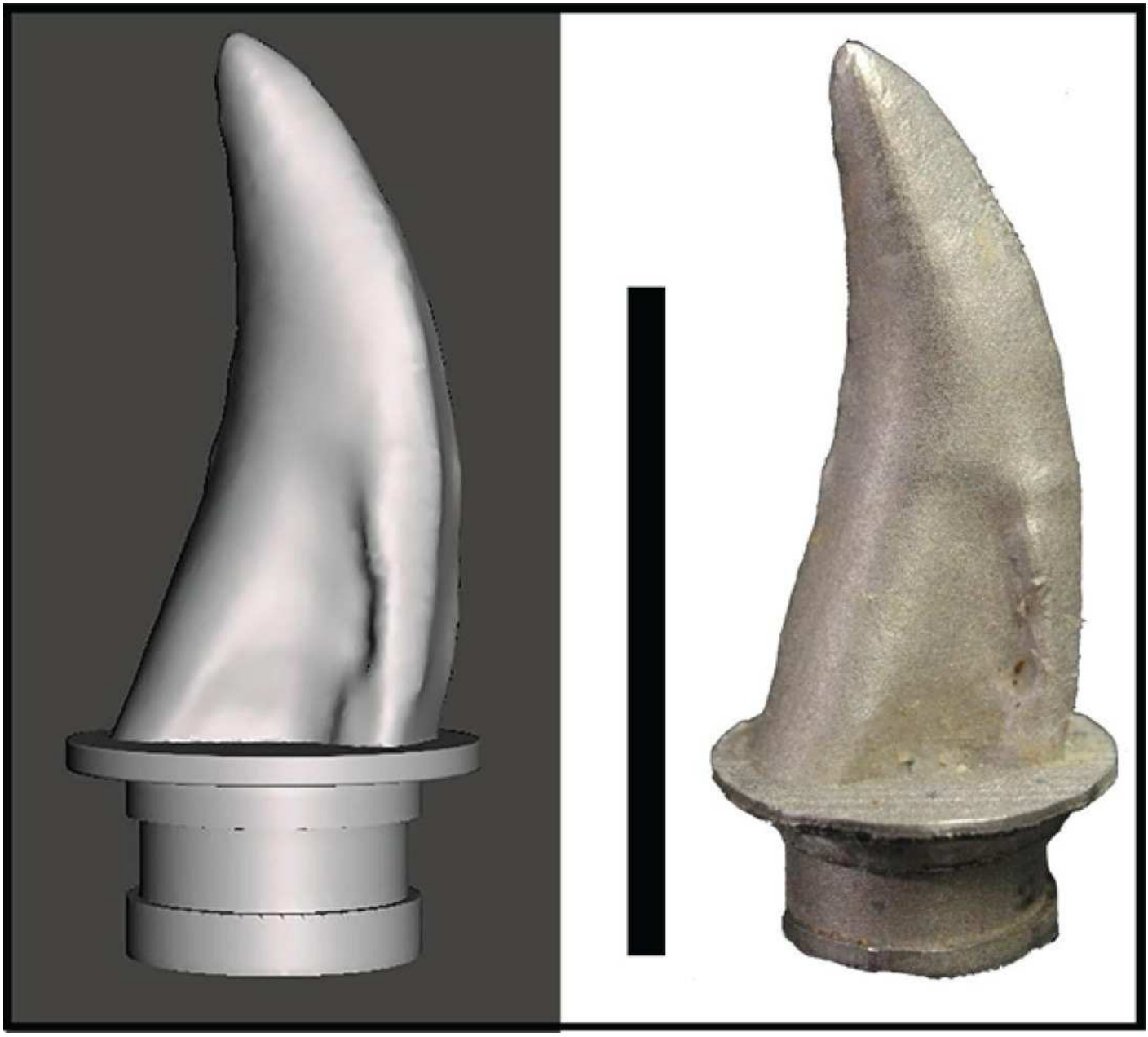

# Figure 4

Spatial maps showing experimental indentation locations on bovine long bones.

A) Right humerus, B) left radius and ulna.

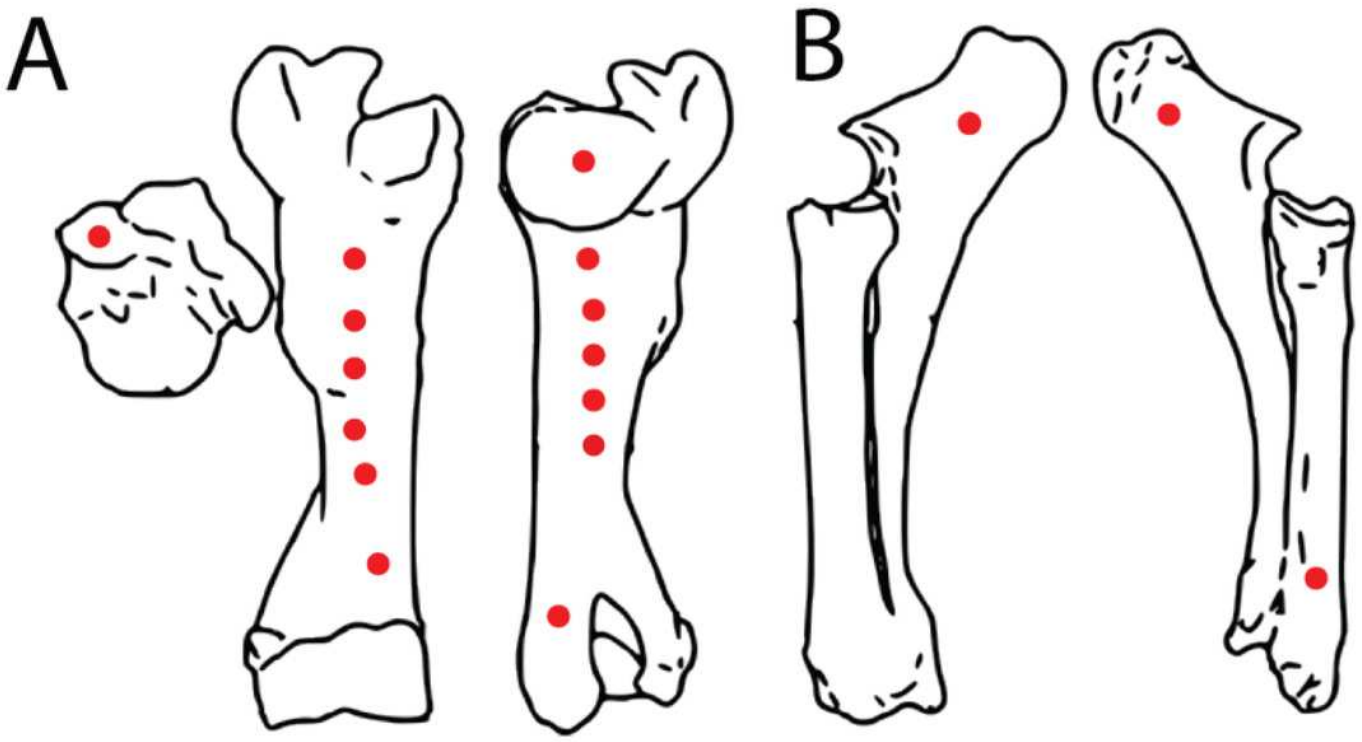

# Figure 5

Computed tomographic image of bovine right humerus post-indentation.

Computed tomographic image of bovine right humerus post-indentation. Red arrows indicate location of experimental indentations.

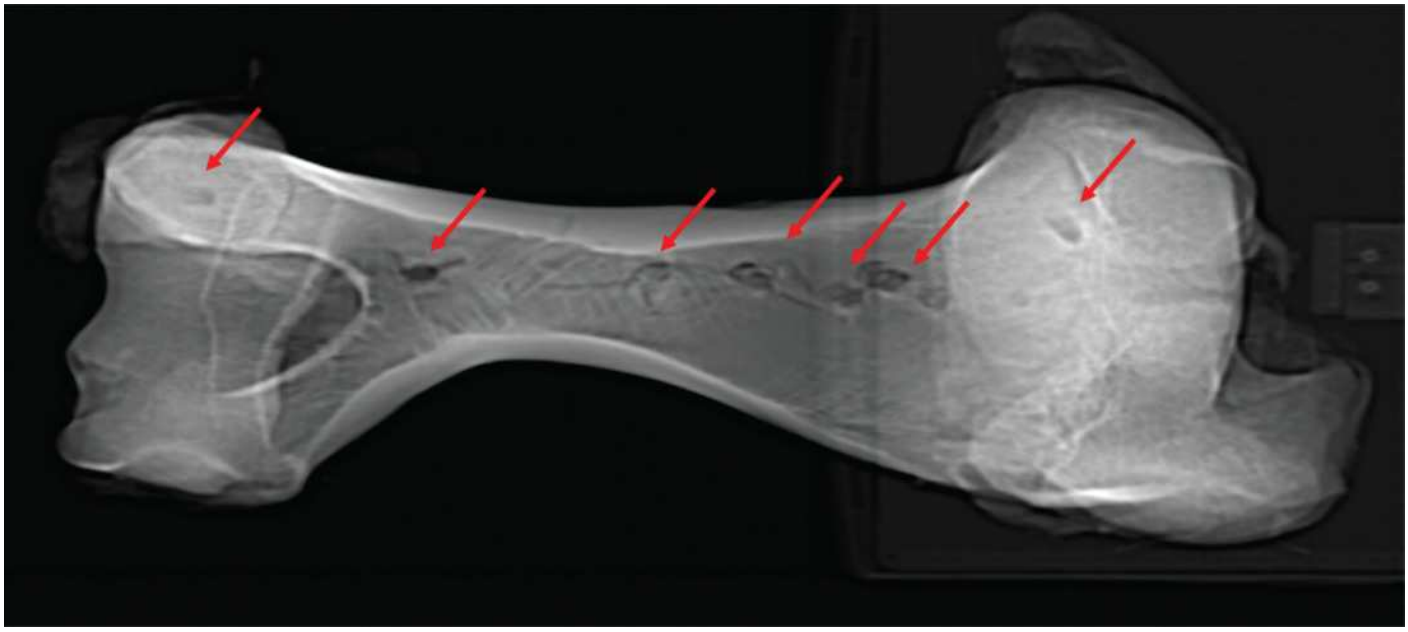

# Figure 6

Indentation force-cortical thickness plots for experimental data.

Indentation force-cortical thickness plots for experimental data. Thick line represents the fitted linear regression line. Shaded region represents 95% confidence intervals. (A) Analysis done using full dataset that excluded trials with evidence of bone fractures. (B) Analysis excluding both indentation forces at or over the 10,000 N threshold, and those trials that showed evidence of fracture.

A

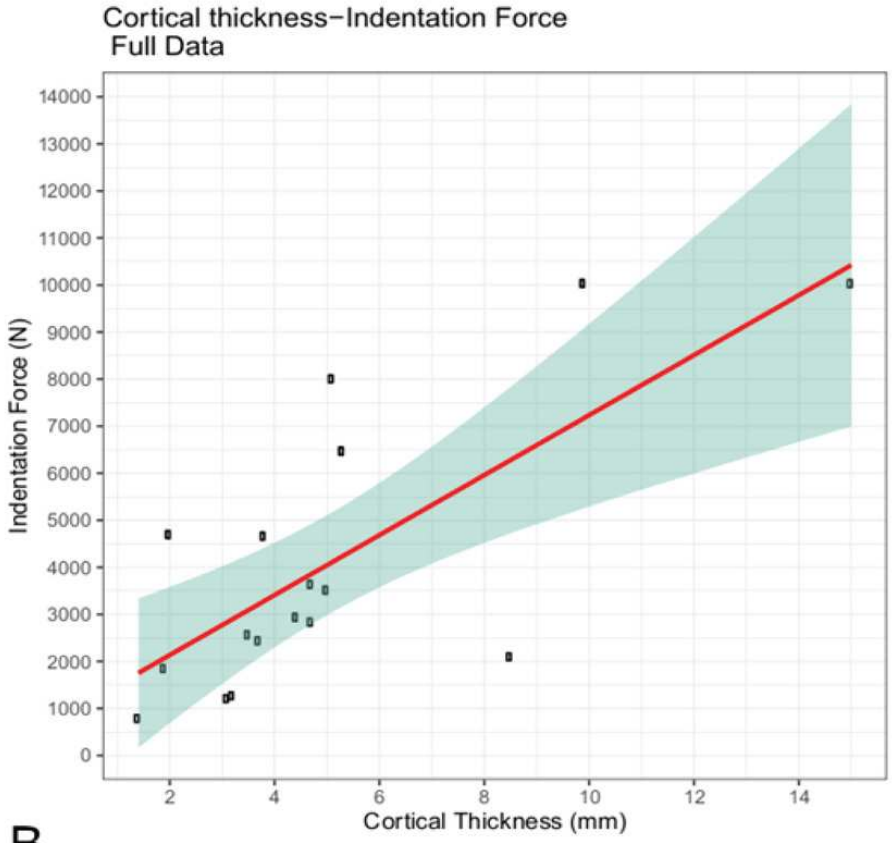
Cortical thickness−Indentation Force
Full Data
Indentation Force (N)
Cortical Thickness (mm)

B

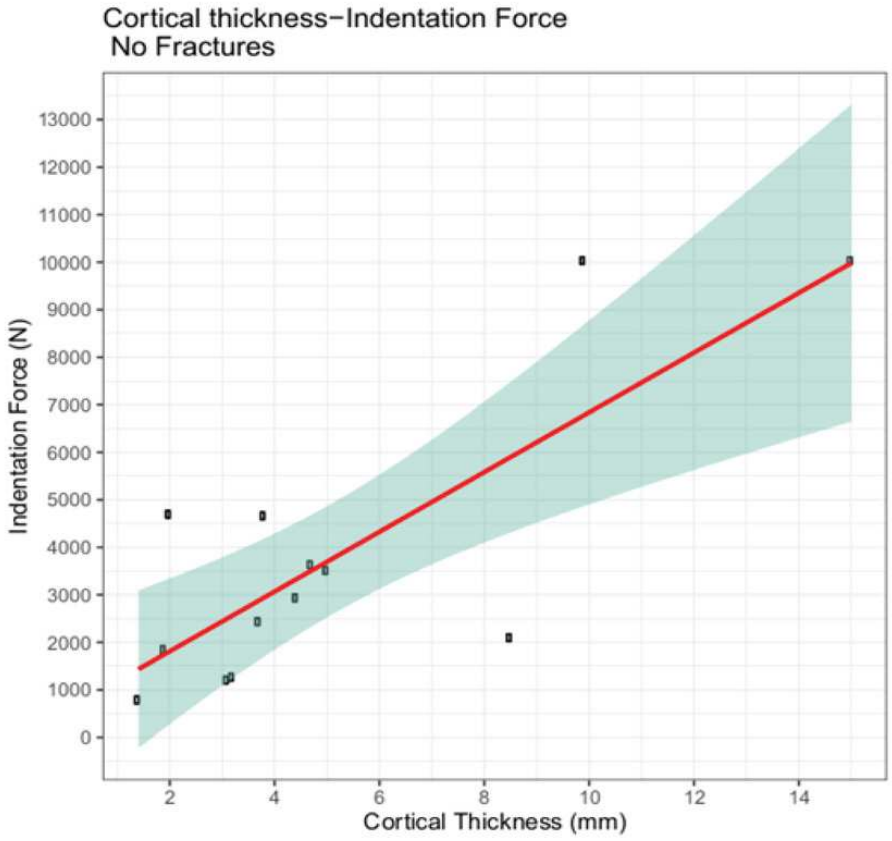
Cortical thickness−Indentation Force
No Fractures
Indentation Force (N)
Cortical Thickness (mm)

## Table 1(on next page)

Puncture dimensions (mm), cortical thickness (mm), and measured force (N) of the 17 indentation trials.

**Table 1: Puncture dimensions (mm), cortical thickness (mm), and measured force (N) of the 17 indentation trials.**

| Puncture Dimensions (mm) | | | Cortical Thickness | Force |
|---|---|---|---|---|
| Length | Width | Depth | (mm) | (N) |
| 11 | 7.7 | 10 | 1.4 | 782.929 |
| 7.3 | 5.7 | 10 | 1.9 | 1844.92 |
| 9.5 | 8 | 10 | 2 | 4690.79 |
| 10 | 8.1 | 10 | 3.1 | 1202.62 |
| 6.9 | 5.2 | 6.8 | 3.2 | 1263.62 |
| 6.7 | 4.1 | 1 | 3.5 | 2562.17 |
| 8.8 | 5.2 | 10 | 3.7 | 2432.3 |
| 10.4 | 5.4 | 10 | 3.8 | 4657.54 |
| 2.8 | 3.7 | 4 | 4.42 | 2931 |
| 8.3 | 5.7 | 10 | 4.7 | 2830.95 |
| 8.4 | 5 | 10 | 4.7 | 3630.72 |
| 9.3 | 5.3 | 10 | 5 | 3509 |
| 8.8 | 5.3 | 10 | 5.1 | 8000 |
| 8.5 | 5.6 | 10 | 5.3 | 6463.85 |
| 11.9 | 3.8 | 4 | 8.5 | 2094.83 |
| 6 | 3.4 | 8.5 | 9.9 | 10028.7 |
| 5 | 5.6 | 7.9 | 15 | 10024.6 |